Electronic Supplementary Material (ESI) for Journal of Materials Chemistry A.

Supplemenary Information

Excellent *ZT* achieved in $Cu_{1.8}S$ thermoelectric alloys through introducing rare-earth trichlorides

Zhen-Hua Ge, Yi-Xin Zhang, Dongsheng Song, Xiaoyu Chong, Peng Qin, Fengshan Zheng, Jing Feng* and Li-Dong Zhao**

1. Experimental section

$Cu_{1.8}S$ powder was fabricated by using pure elemental powder (99.99% Cu (under 200 mesh), 99.95% S (under 200 mesh)) as raw materials. After weighing by stoichiometry, the powders were contained in stainless-steel vessels and balls, in which the weight ratio of ball to powder was kept at 20:1, and the ball-milling (QM-4F, Nanjing University, China) was executed at 425 rpm for 3 h under the protective gases condition with high-purity nitrogen (95%) and hydrogen (5%). Then the synthetic powder was fully mixed with $RECl_3$ (RE: Y, La, Pr, Nd, Ce) powder (>99.9%) through manual grind by using agate mortar and pestle for 30 minutes. Considering for the hygroscopic nature of the chloride and the possibility of the oxidation reaction during the manual grinding, the procedure for mixing powder was operated in the glove box. Subsequently, the mixed powders were sintered at 723 K for 5 min in a φ15 mm graphite mold under axial compressive stress 50 MPa in vacuum using a spark plasma sintering (SPS) system (Sumitomo SPS1050, Japan). The sintered specimens were disk-shaped with dimensions of 15 mm × 4 mm.

The integral specimens were polished to check phase impurity on X-ray diffraction (XRD Bruker D8, Germany) with Cu Kα radiation (λ=1.54Å) at first. Then each sample was cut and grinded into two specimens shaped like bars and coins, respectively. The size of the former one is required as 12 mm × 3 mm × 3 mm for measurement of electrical resistance and Seebeck coefficient, which used ZEM-3 (Ulvac-Riko, Japan) system under a helium atmosphere from room temperature to 773 K. The later one was sized as $\varphi \approx 6$ mm and 1−2

mm thickness for thermal properties measurements, in which thermal conductivity κ of the specimens was calculated by the relationship $\kappa=DC_p\rho$, where thermal diffusivity D was measured by laser flash method (NETZSCH, LFA457, Germany), and the specific heat capacity C_p was indirectly obtained using a representative sample (Pyroceram 9606) in the range 323-773 K, while the mass density of the samples was simply measured by the Archimedes principle. Besides, the microstructure was observed by field emission scanning electron microscopy. Besides, the Hall carrier concentration (n_H), and carrier mobility (μ_H) of the samples were measured at room temperature by a Hall effect measurement system (Ecopia, HMS-7000, Korea). A magnetic field of 0.545T and an electrical current of 1 μA were applied. Lattice parameters were calculated by Jade software, the calculated errors for the lattice parameter along *a* and *c* axis are 0.02%-0.08% and 0.03-0.10%, respectively, the cell volume is around 0.11%-0.15%.

$LaCl_3$ was selected to be the most effective dopant in $Cu_{1.8}S$ due to the best TE performance of this series of materials. The doping content has been adjusted during the preparation, simultaneously, phase purity, microstructure, electrical and thermal properties were be measured under the same measurement conditions mentioned above. And scanning transmission electron microscopy (STEM, Phililp, Tecnai F20, Amsterdam, Dutch) was extra used to investigated more details of microstructure, conventional methods such as cutting, grinding, dimpling, polishing were used to prepare the thin TEM specimens. An energy dispersive X-ray spectrometer (EDS) was utilized to detect the composition and content of the elements.

2. Lattice parameters from XRD for $Cu_{1.8}S$ with $RECl_3$ doping

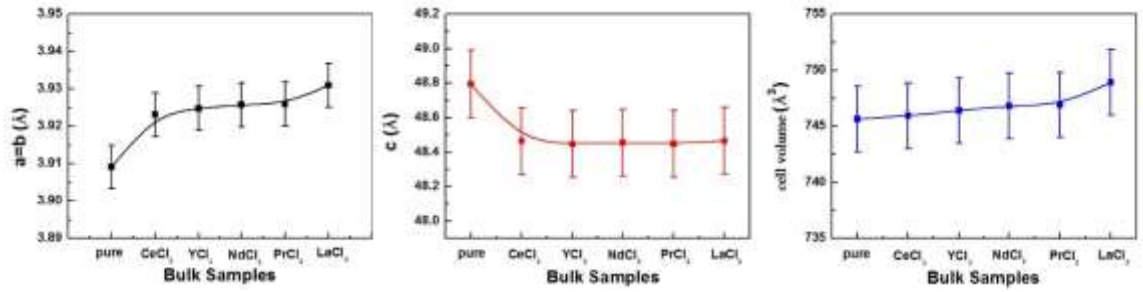

Figure S1 The lattice parameters of $Cu_{1.8}S$ with different dopants

3. Microstructure of $Cu_{1.8}S$ with $RECl_3$ samples

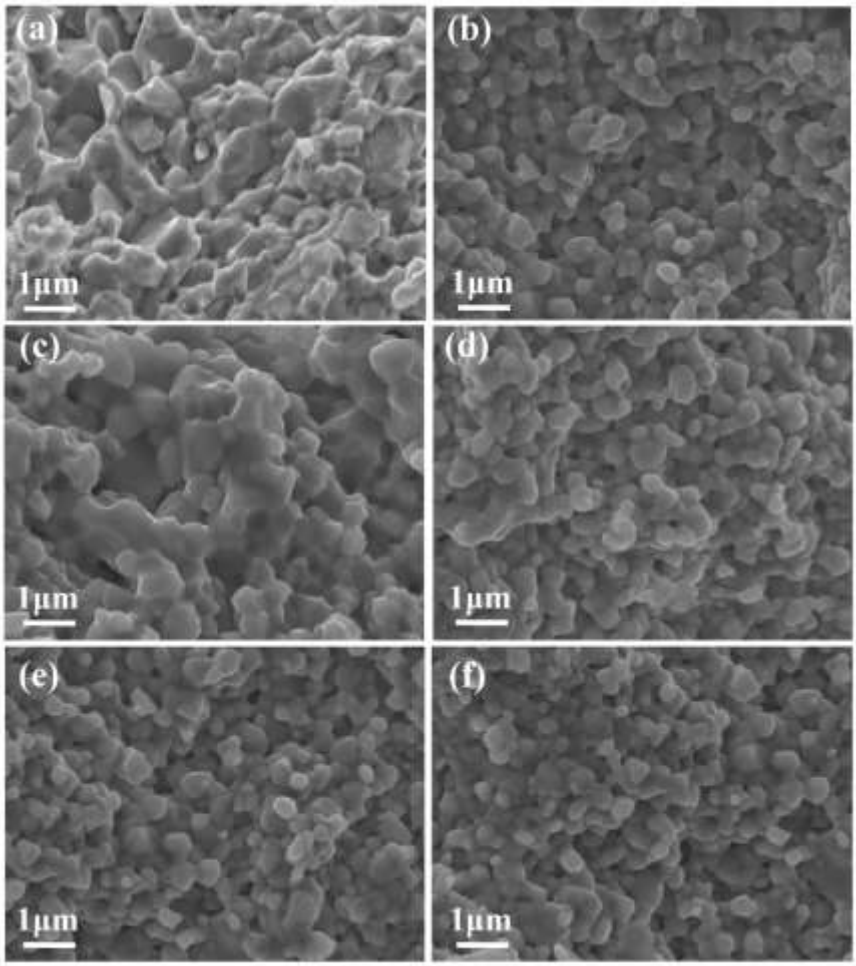

Figure S2 The SEM images of fractured $Cu_{1.8}S$ + 1% $RECl_3$ (RE=Y, La, Pr, Nd, Ce) samples, undoped $Cu_{1.8}S$ (a), with $CeCl_3$ (b), YCl_3 (c), $NdCl_3$ (d), $PrCl_3$ (e), and 1% $LaCl_3$ (f).

4. Calculated cell volume from XRD for $Cu_{1.8}S$ with $LaCl_3$ doping

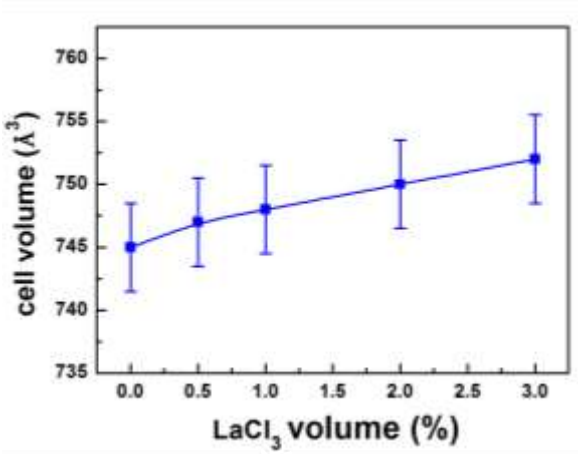

Figure S3 The lattice parameters of $Cu_{1.8}S$ with different $LaCl_3$ contents.

5. Microstructure of $Cu_{1.8}S$ with $LaCl_3$ samples

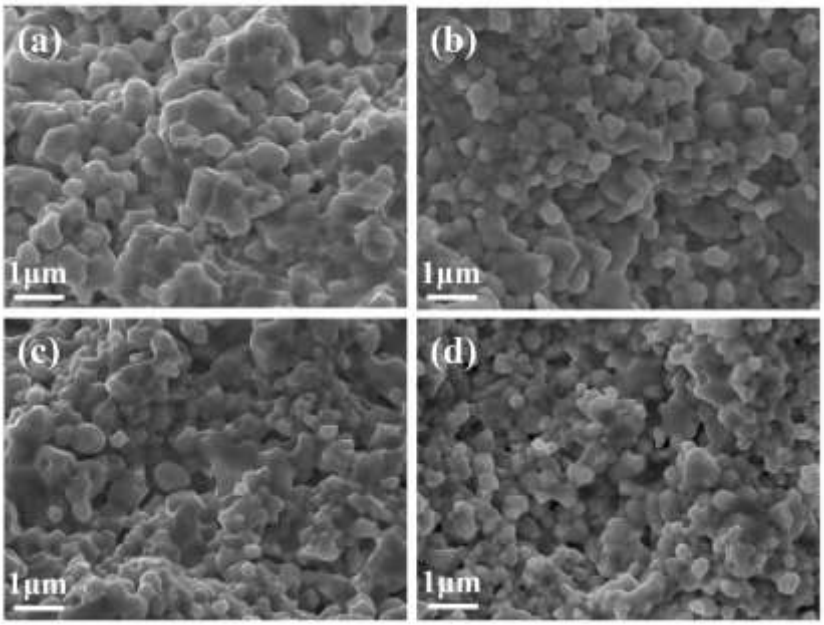

Figure S4 The SEM images of fractured $Cu_{1.8}S$ + x% $LaCl_3$ (x= 0.5, 1, 2, 3) bulk samples, x=0.5 (a), x=1 (b), x=2 (c), and x=3 (d).

6. Method of calculations

The calculations for electronic structures are performed based on the density functional theory (DFT) as implemented in the CASTEP code[1,2]. The Heyd-Scuseria-Ernzerh of hybrid functional (HSE06)[3,4] is used in this work, which adopts a screened Coulomb potential and greatly improves the description of band structures, including band gaps. The interactions between the ionic cores and the valence electrons were indicated by Ultrasoft pseudo-potentials (USPPs). A plane wave expansion method was applied for the optimization of the crystal structure. A special k-point sampling in the first irreducible Brillouin zone was

confirmed by the Monkhorst–Pack scheme, and the *k* point mesh was selected as 10×10×10. A kinetic energy cut-off value of 400.0 eV was used for the plane wave expansion in reciprocal space. So the selected values are suitable for the chosen system. The Broyden–Fletcher–Goldfarb–Shannon (BFGS) method was applied to relax the whole structure based on total energy minimization. The total energy changes during the optimization processes were finally converged to 1×10^{-6} eV and the forces per atom were reduced to 0.05 eV·Å^{-1}.

The original configuration of cubic chalcocite is taken from Ref. [5]. For the digenite $Cu_{1.8}S$, the cell can be constructed by having a 2×2×2 cubic chalcocite Cu_2S supercell with 6 Cu vacancies. In this supercell, 58 Cu atoms occupy the 8c, 4b, and 192l Wyckoff sites, and 32 S atoms occupy the 4b Wyckoff sits. Monte Carlo method is used to search the possible structures and only the structures with lowest total energy are considered as the most plausible digenite structures[4]. We note that the fully optimized structures of digenite $Cu_{1.8}S$ are slightly distorted from the original crystal symmetry because of the small cell size and partial occupation of the Wyckoff sites by randomly distributed Cu atoms. In order to reproduce the experimentally observed ratios of La doped $Cu_{1.8}S$, two La ions occupy the Cu sites in a super cell with 90 atoms.

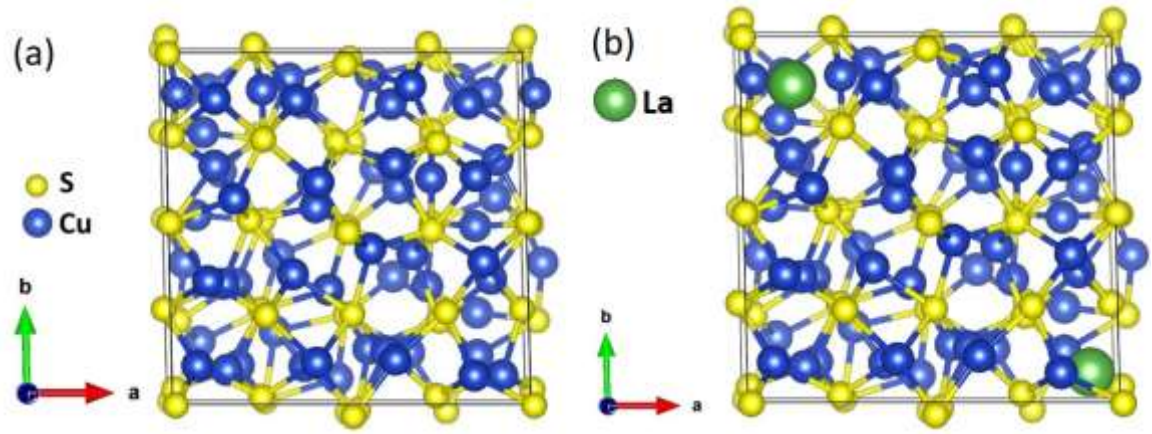

Figure S5 The crystal structures and calculated band structures of pure $Cu_{1.8}S$ ((a) and (b))

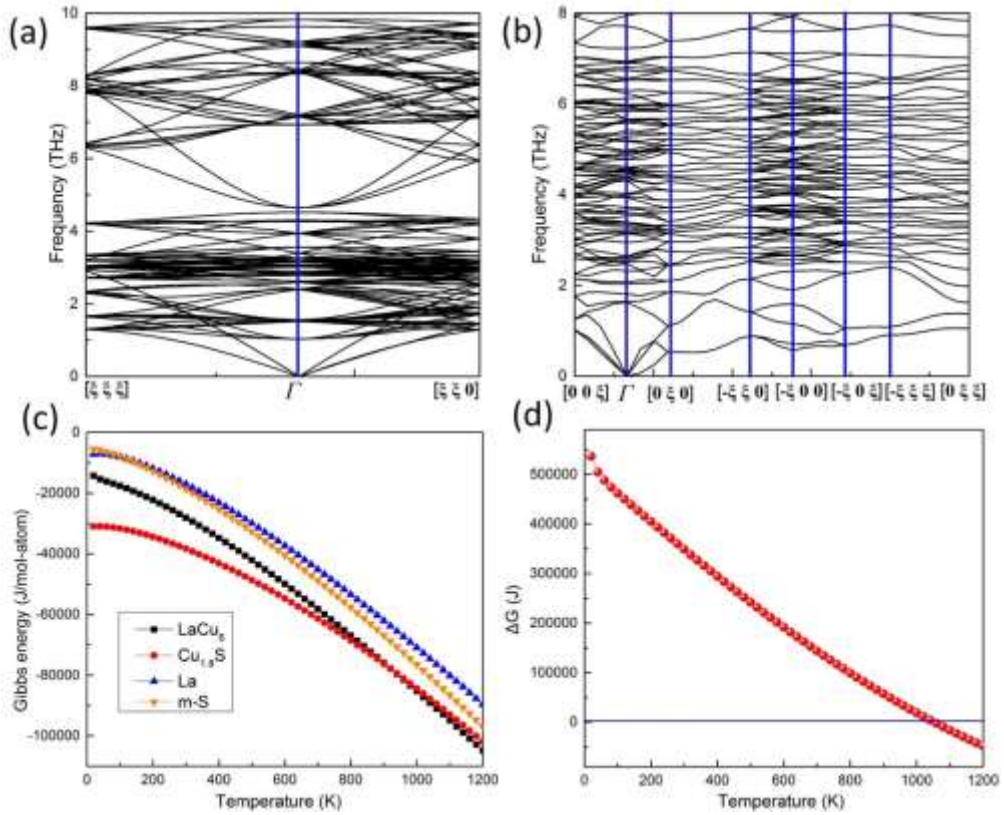

Figure S6 The phonon dispersion of $Cu_{1.8}S$ (a) and $LaCu_6$ (b). Gibbs energy for $Cu_{1.8}S$, $LaCu_6$, La and monoclinic S (c) and reaction Gibbs energy difference (ΔG) for the formation of $LaCu_6$ (d).

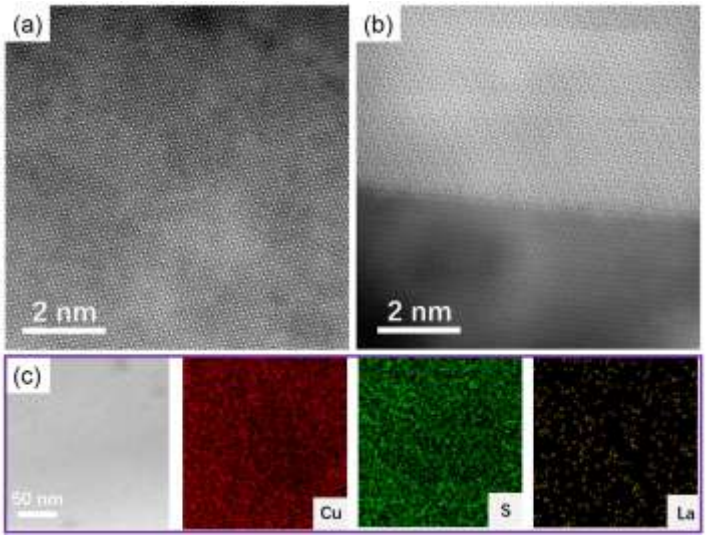

Figure S7 (a, b) High-resolution STEM HAADF images of $Cu_{1.8}S$+2%$LaCl_3$ bulk sample and (c) TEM-EDS image of $Cu_{1.8}S$+2%$LaCl_3$ bulk sample.

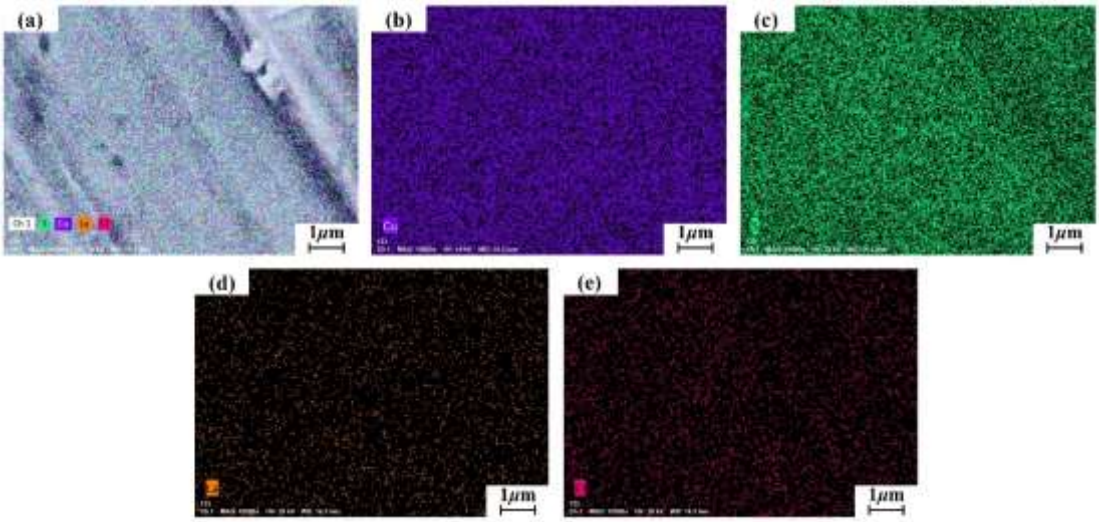

Figure S8 SEM images of p-type polycrystalline $Cu_{1.8}S$ with 2 *wt.* % $LaCl_3$ the elemental distribution for Cu, S, La and Cl (a), the elemental distribution for Cu (b), the elemental distribution for S (c), the elemental distribution for La (d) and the elemental distribution for Cl (e).

Table S1 The measrued densisity, relative density, carrier concentration and mobility of $Cu_{1.8}S$ bulk with different dopants.

Bulk sample	Measured density (gcm^{-3})	Relative density (%)	Hall carrier concentration n_H (10^{20} cm^{-3})	Hall carrier mobility μ_H (cm^2/sec)
Cu1.8S	5.36	95.71	4.02	33
+1% $CeCl_3$	5.44	97.14	3.11	26
+1% YCl_3	5.52	98.57	3.04	24
+1% $NdCl_3$	5.23	93.39	3.60	28
+1% $PrCl_3$	5.33	95.17	3.28	31
+1% $LaCl_3$	5.39	96.25	3.43	25

Reference

1 P. Hohenberg and W. Kohn, *Phys. Rev. B*, 1964, **136**, 864.

2 M. Segall, P. Lindan, M. Probert, C. Pickard, P. Hasnip, S. Clark, and M. Payne, *J. Phys.: Condens. Matter.*, 2002, **14**, 2717.

3 G. Kresse and J. Furthmüller, *Phys. Rev. B*, 1996, **54**, 11169-11186.

4 G. Kresse and D. Joubert, *Phys. Rev. B*, 1999, **59**, 1758-1775.

5 R. W. Potter, Econ. Geol., 1977, 72, 1524.